AD-A009 208

A CALCULATIONAL MODEL FOR HIGH ALTITUDE EMP

Louis W. Seiler, Jr.

Air Force Institute of Technology
Wright-Patterson Air Force Base, Ohio

March 1975

DISTRIBUTED BY:

NTIS

National Technical Information Service
U. S. DEPARTMENT OF COMMERCE

UNCLASSIFIED
SECURITY CLASSIFICATION OF THIS PAGE (When Data Entered)

REPORT DOCUMENTATION PAGE		READ INSTRUCTIONS BEFORE COMPLETING FORM
1 REPORT NUMBER AFIT/EN/PH/75-13	2 GOVT ACCESSION NO	3 RECIPIENT'S CATALOG NUMBER AD-A009 208
4 TITLE (and Subtitle) A CALCULATIONAL MODEL FOR HIGH ALTITUDE EMP		5 TYPE OF REPORT & PERIOD COVERED MS Thesis 6 PERFORMING ORG. REPORT NUMBER
7 AUTHOR(s) Louis W. Seiler, Jr. Capt USAF		8 CONTRACT OR GRANT NUMBER(s)
9 PERFORMING ORGANIZATION NAME AND ADDRESS Air Force Institute of Technology (AFIT-ENP) Wright-Patterson Air Force Base, Ohio 45433		10 PROGRAM ELEMENT, PROJECT, TASK AREA & WORK UNIT NUMBERS
11 CONTROLLING OFFICE NAME AND ADDRESS Air Force Weapons Laboratory (DYT) Kirtland AFB, New Mexico 87115		12 REPORT DATE March 1975 13 NUMBER OF PAGES 81 60
14 MONITORING AGENCY NAME & ADDRESS, if different from Controlling Office) Air Force Institute of Technology (AFIT-ENP) Wright-Patterson Air Force Base, Ohio 45433		15 SECURITY CLASS (of this report) UNCLASSIFIED 15a DECLASSIFICATION DOWNGRADING SCHEDULE

16 DISTRIBUTION STATEMENT (of this Report)

Approved for public release; distribution unlimited.

17 DISTRIBUTION STATEMENT (of the abstract entered in Block 20, if different from Report)

18 SUPPLEMENTARY NOTES

Approved for public release, IAW AFR 190-17
Jerry C. Hix Captain, USAF
Director of Information

19 KEY WORDS (Continue on reverse side if necessary and identify by block number)
EMP
High Altitude EMP
Electromagnetic Pulse
EMP Model

Reproduced by
NATIONAL TECHNICAL INFORMATION SERVICE
US Department of Commerce
Springfield, VA 22151

20 ABSTRACT (Continue on reverse side if necessary and identify by block number)

An electromagnetic pulse (EMP) model is developed which allows a quick computation of the time development of the electric fields generated by a high altitude nuclear burst. The model is based on the Karzas-Latter high frequency approximation for high altitude EMP, which describes fields generated by Compton electrons interacting with the earth's magnetic field. The proper choice of a gamma time output function, which can be integrated in closed form, and a small angle approximation, made in the expressions for the Compton currents and air conductivity, eliminate the time consuming numerical integrations usually

DD FORM 1 JAN 73 1473 EDITION OF 1 NOV 65 IS OBSOLETE

UNCLASSIFIED
SECURITY CLASSIFICATION OF THIS PAGE (When Data Entered)

necessary in EMP models to compute the Compton currents and air conductivity. This results in a considerable savings in computation time. The model is presented in a manner which is simple to use but still allows the variation of the major theoretical parameters in the problem. A simplified model of electron collision frequency as a function of electric field strength is given which enables the model to predict accurate results for nuclear weapon gamma yields up to at least 100 Kt. The results predicted by this EMP model compare to within 5.5% with results from the Air Force Weapons Laboratory CHEMP computer code. The computation time using the presented model on a CDC 6600 computer is typically 5 sec or less for a 5 shake computation period in steps of .1 shake. The model presented should be useful for both classroom instruction and nuclear vulnerability/survivability studies and analysis problems.

A CALCULATIONAL MODEL FOR HIGH ALTITUDE EMP

THESIS

GEP/PH/75-13

Louis W. Seiler, Jr.
Captain USAF

DDC
RECEIVED
MAY 6 1975
B

Approved for public release; distribution unlimited.

iia.

A CALCULATIONAL MODEL FOR HIGH ALTITUDE EMP

THESIS

Presented to the Faculty of the School of Engineering

of the Air Force Institute of Technology

Air University

In Partial Fulfillment of the

Requirements for the Degree of

Master of Science

by

Louis W. Seiler, Jr., B.S.
Captain USAF

Graduate Engineering Physics

March 1975

Approved for public release; distribution unlimited.

IIXC

Preface

I would like to express my appreciation to my advisor, Major Carl T. Case, for his patient guidance and understanding during the work on this thesis. His advice was a major contribution towards the completion of this work.

I am also gratefully indebted to Captain Leon A. Wittwer of the Air Force Weapons Laboratory for his enlightening insights into the finer aspects of the high altitude EMP problem.

I would also like to thank Captain Terry C. Chapman for his time in discussing various concepts and ideas with me.

A large amount of my thanks must go to my wife, Joan. Without her patient understanding, moral support, and encouragement, this thesis could not have been completed.

Louis W. Seiler, Jr.

Contents

Page

Preface ii

List of Figures iv

Abstract v

I. Introduction 1

II. Theory 4

Overview 4
Particle Densities 4
Currents and Conductivity 8
Field Equations 12

III. Model Considerations 15

General 15
Time Dependence of Gamma Rays 15
Energies 17
Compton Electron Lifetime 22
Small Angle Approximation 22
Electron Collision Frequency 23
Preionization 25
Calculation Method 26

IV. Results 29

V. Conclusions and Recommendations 40

Uses 40
Limitations 41
Recommendations 41

Bibliography 43

Appendix A: HAEMP Model Summary 44

Vita 51

List of Figures

Figure		Page
1	Model Geometry	5
2	Typical Long Gamma Output Pulse	18
3	Typical Narrow Gamma Output Pulse	19
4	Peak Electric Field Values for 100 Km Burst Heights	30
5	Electric Field Development for .25 Kt Gamma Burst	32
6	Peak Electric Field as a Function of Burst Height	33
7	Peak Electric Fields for Two Gamma Pulse Shapes	34
8	Effect of a .03 Kt Gamma Yield Precursor Burst	36
9	Effect of Geomagnetic Field Strength on Peak Fields	38

Abstract

An electromagnetic pulse (EMP) model is developed which allows a quick computation of the time development of the electric fields generated by a high altitude nuclear burst. The model is based on the Karzas-Latter high frequency approximation for high altitude EMP, which describes fields generated by Compton electrons interacting with the earth's magnetic field. The proper choice of a gamma time output function, which can be integrated in closed form, and a small angle approximation, made in the expressions for the Compton currents and air conductivity, eliminate the time consuming numerical integrations usually necessary in EMP models to compute the Compton currents and air conductivity. This results in a considerable savings in computation time. The model is presented in a manner which is simple to use but still allows the variation of the major theoretical parameters in the problem.

A simplified model of electron collision frequency as a function of electric field strength is given which enables the model to predict accurate results for nuclear weapon gamma yields up to at least 100 Kt. The results predicted by this EMP model compare to within 5.5% with results from the Air Force Weapons Laboratory CHEMP computer code.

The computation time using the presented model on a CDC 6600 computer is typically 5 sec or less for a 5 shake computation period in steps of .1 shake.

The model presented should be useful for both classroom instruction and nuclear vulnerability/survivability studies and analysis problems.

A CALCULATIONAL MODEL FOR HIGH ALTITUDE EMP

I. Introduction

In recent years there has been a growing concern about the nuclear weapon effect known as the electromagnetic pulse or the EMP. As the theory of EMP developed it was realized that there are actually several types of EMP which are characterized by the mechanisms which produce them. Types of EMP include surface EMP, system generated EMP (SGEMP), and high altitude EMP. A comprehensive discussion of the various types of EMP is presented by Kinsley (Ref 1). This report will address only one of these, that of high altitude EMP.

The EMP is basically a long range nuclear weapons effect wherein a high intensity electromagnetic field is radiated over a wide frequency band. The duration of this pulse is typically on the order of shakes (1 shake = 10^{-8} sec). Specifically, high altitude EMP is that produced by a nuclear detonation above 20 Km.

The high altitude EMP problem is a subject of great interest to the USAF due to its long range nature, and much effort goes into predicting the time development of the fields. These high intensity EMP fields present a potential threat to weapons systems which rely on electrical or electronic components, such as communications, electronic counter measures (ECM), navigation, guidance, reconnaissance, and many others. The threat levels predicted by theoretical models have a direct impact on the design of future Air Force weapons systems. These threat levels also help to predict the survivability of present weapons systems.

The EMP generation models currently in use by the Air Force Weapons Laboratory (AFWL), are highly sophisticated and use large amounts of computer time. Other models available are very simple and give essentially order of magnitude results. The model presented in this report is intended to provide an alternative between these extremes, giving results close to those of the more advanced AFWL models but with very short expenditures of computer time. One important capability of this model is its ability to account for a preionization level due to a precursor burst.

This model should be useful for quickly obtaining a meaningful estimate of the EMP environment for parameter variation or for use in a classroom situation to give a feel for the calculations involved in predicting the generated EMP fields and showing the effects of a given parameter.

The theory behind the high altitude EMP model presented is based on that of Karzas and Latter (Ref 2). Basically the Karzas-Latter theory states that prompt gamma rays from the weapon produce Compton electrons within a specified region of the atmosphere known as the absorption region. These Compton electrons are turned by the magnetic field of the earth to produce the radiated electromagnetic fields.

There are several assumptions which are basic to the Karzas-Latter model. These assumptions are: the earth's magnetic field is assumed to be uniform, the magnetic field lines have no curvature in the gamma ray absorption layer, the earth's surface is assumed to be flat, the gamma rays are monoenergic, each gamma interacts with the atmosphere to produce only one forward directed Compton electron, the Compton electrons produced are also considered to be monoenergic and have a constant

velocity throughout their lifetime, and only the high frequency portion of the pulse is considered.

One additional approximation is made in this study. This is a small angle approximation in the trigonometric expressions for the Compton currents and air conductivity. This approximation, with the judicious choice of a function to represent the time dependence of the weapon yield, leads to closed form expressions for the Compton currents and air conductivity. This saves considerable computation time and greatly simplifies the calculations. For this approximation to be valid the cyclotron frequency ω of the Compton electrons in the geomagnetic field must be small enough so that the small angle approximations for $\sin \omega t$ and $\cos \omega t$, where t is in seconds, are valid.

In all cases where quantities vary with the atmospheric density, an exponential atmosphere model is used.

Factors not considered in the model are recombination of ions, avalanching or cascading of secondary electrons, X-ray effects, and self-consistent electromagnetic fields.

II. Theory

Overview

Since the solution to the EMP problem is actually the solution of a classical electromagnetic theory problem, the derivation of the model equations reduces to putting Maxwell's equations into a convenient form. This is essentially accomplished by expressing Maxwell's equations in spherical coordinates and transforming to a retarded time frame. One must also develop expressions for the currents and conductivities of the system in the absorption region. The general equations describing the high altitude model of Karzas and Latter have been derived in great detail by Chapman (Ref 3). Only the major points of the derivation will be given here. The system origin is assumed to be at the burst point with detonation at time t = 0. This geometry is illustrated in Fig. 1.

The key points to be remembered in this model are:

1. Each gamma ray gives rise to one downward traveling Compton electron.
2. The electrons are turned by the earth's magnetic field giving rise to a centrifugal acceleration.
3. The relativistic electrons radiate energy in their forward direction.
4. The gamma rays and the EMP radiation travel at the same speed. This leads to constructive interference of the radiation from each of the electrons.

Particle Densities

The gamma rays from the nuclear weapon travel in a straight line to a point where they produce Compton electrons. At any given point r

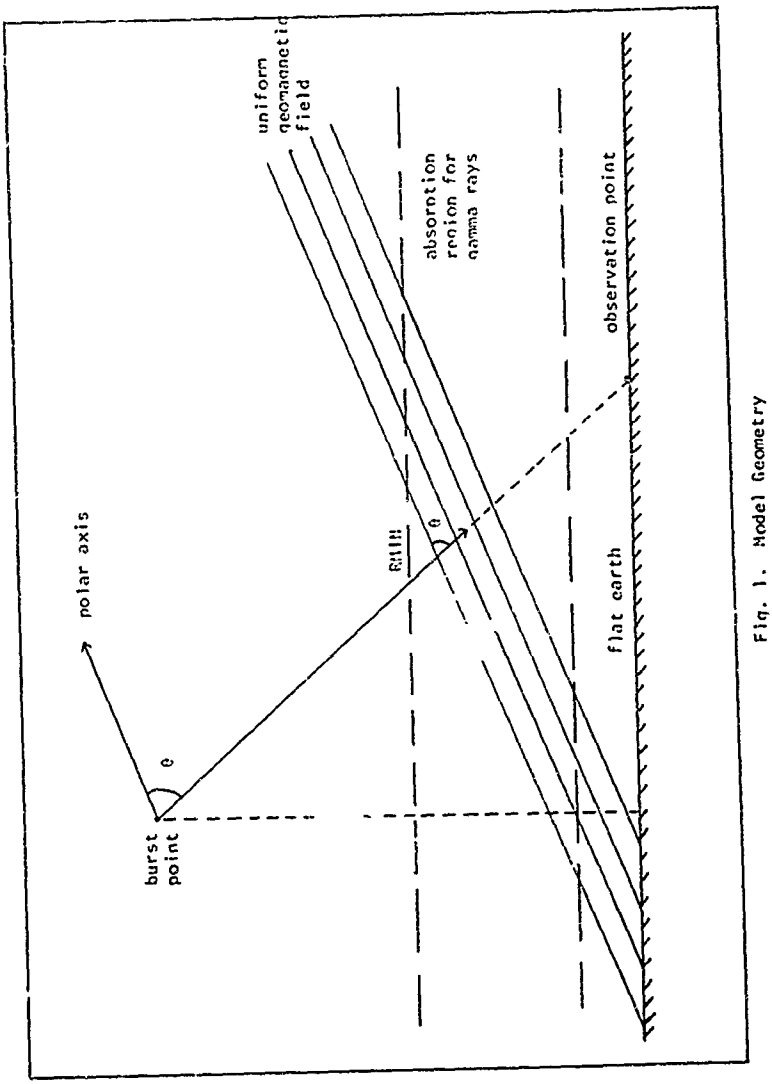


Fig. 1. Model Geometry

the number of gammas which interact to produce Compton electrons is

$$g(r) = \frac{Y}{E} \frac{\exp\left[-\int_0^r \frac{dr'}{\lambda(r')}\right]}{4\pi r^2 \lambda(r)} \qquad (1)$$

where $\lambda(r)$ is the mean free path of gamma rays to produce Compton electrons, Y is the gamma yield of the weapon in electron volts (eV), and E is the mean gamma energy in eV.

Equation (1) may also be called the radial distribution function, or an attenuation function for interacting gamma rays. The $\frac{Y}{E}$ term is the total number of gamma rays available from the weapon. The $4\pi r^2$ term accounts for the divergence of the gamma rays as the radius r is increased while the remaining terms account for the reduction in gammas due to their absorption in the atmosphere, based on the mean free path.

It is assumed that the gamma mean free path varies as the exponential atmosphere. This gives the functional relationship between λ and r:

$$\lambda(r) = \lambda_0 \exp\left[(HOB - r \cos A)/S\right] \qquad (2)$$

where

λ_0 = gamma mean free path at standard pressure

HOB = height of burst in Km above the earth's surface

r = radial distance from the burst point to the point of interest

A = angle between the position vector $\vec{r}$ and the vertical

S = atmospheric scale height

With this assumption, Eq (1) can be integrated and becomes

$$g(r) = \frac{Y}{E} \frac{1}{4\pi r^2 \lambda(r)} \exp\left\{-\frac{S}{\lambda_0 \cos A} \exp\left(-\frac{HOB}{S}\right)\left[\exp\left(\frac{r \cos A}{S}\right) - 1\right]\right\} \qquad (3)$$

Now if f(t) is the time distribution function of the weapon yield, the rate of Compton electrons, n_c, produced at a given point r and time t is given by

$$\frac{dn_c}{dt} = g(r)\, f\left(t - \frac{r}{c}\right) \tag{4}$$

Each Compton electron produces through inelastic scattering events several secondary electrons which form the basis for the conductivity of the atmosphere. As in the Karzas-Latter approach, each Compton electron is assumed to have a constant speed, V_o, throughout the range, R, of the electron which is a function of altitude. This allows the lifetime to be expressed as R/V_o. If each Compton electron produces secondary electrons at a constant rate, the rate of secondary electron, n_s, production is

$$\frac{dn_s}{dt} = \frac{E_c/33\ eV}{R/V_o}\, n_c \tag{5}$$

where E_c is the energy of the Compton electron and 33 eV is the average ionization energy per air molecule (Ref 2).

Considering the differential current produced by the Compton electrons, it can be shown (Ref 3) that the Compton current and the number of Compton electrons are given by

$$\vec{J}^c(\tau) = -\, e\, g(r) \int_0^{R/V_o} V(\tau')\, f\left(\tau - \tau' + \frac{X(\tau')}{c}\right) d\tau' \tag{6}$$

$$n_c(\tau) = g(r) \int_0^{R/V_o} f\left(\tau - \tau' + \frac{X(\tau')}{c}\right) d\tau' \tag{7}$$

where

$$\tau = t - \frac{r}{c}$$

τ' = the time since the creation of the Compton electron

$X(\tau')$ = the radial distance the Compton electron has traveled

e = the magnitude of the electron charge

The quantity τ is generally known as retarded time.

It then follows from Eqs (4) and (7) that the number of secondary electrons is

$$n_s(\tau) = \frac{qV_o}{R} g(r) \int_{-\infty}^{\tau} \left[\int_{0}^{R/V_o} f\left(\tau' - \tau'' + \frac{X(\tau'')}{c}\right) d\tau'' \right] d\tau' \qquad (8)$$

where q is $E_c/33$ eV.

Currents and Conductivity

In the Karzas-Latter theory, the speed of the Compton electrons is considered to be a constant, however, there is an acceleration due to the geomagnetic field. The general equation of motion for an electron in this case is

$$\frac{d}{dt} m \gamma \vec{V} = - e (\vec{E} + \vec{V} \times \vec{B}) - m \nu_c \vec{V} \qquad (9)$$

where

m = the electron rest mass

$\vec{V}$ = the electron velocity

$\vec{E}$ = the electric field

$\vec{B}$ = the magnetic field

ν_c = the electron collision frequency

$\gamma = (1 - (V_o/c)^2)^{-\frac{1}{2}}$

If the relativistic motion of the electron is considered, only the V X B term is important and in spherical coordinates, the expressions for the velocity components become (Ref 3)

$$V_r = V_o \ (\sin^2 \theta \cos \omega\tau + \cos^2 \theta) \tag{10}$$

$$V_\theta = V_o \ (\cos \theta \sin \theta \cos \omega\tau - \sin \theta \cos \theta) \tag{11}$$

$$V_\phi = V_o \ (\sin \theta \sin \omega\tau) \tag{12}$$

where ω is the cyclotron frequency for an electron and is given by

$$\omega = \frac{eB_o}{m\gamma} \tag{13}$$

with B_o the magnitude of the geomagnetic field.

From Eq (10), $X(\tau')$ is found to be

$$X(\tau') = V_o \left(\sin^2 \theta \ \frac{\sin \omega\tau'}{\omega} + \tau' \cos^2 \theta \right) \tag{14}$$

The Compton currents may now be written as

$$J_r^c(\tau) = - eg(r) \ V_o \int_o^{R/V_o} [f(T)(\cos^2 \theta + \sin^2 \theta \cos \omega\tau)] \ d\tau' \tag{15}$$

$$J_\theta^c(\tau) = - eg(r) \ V_o \int_o^{R/V_o} [f(T) \sin \theta \cos \theta \ (\cos \omega\tau' - 1)] \ d\tau' \tag{16}$$

$$J_\phi^c(\tau) = - eg(r) \ V_o \int_o^{R/V_o} [f(T) \sin \theta \sin \omega\tau'] \ d\tau' \tag{17}$$

where

$$T = \tau - \left(1 - \frac{V_o}{c}\cos^2\theta\right)\tau' + \frac{V_o}{c}\sin^2\theta\,\frac{\sin\omega\tau'}{\omega} \tag{18}$$

In a similar manner Eq (8) becomes

$$n_s(\tau) = \frac{qV_o}{R}\,g(r)\int_{-\infty}^{T}\left[\int_{o}^{R/V_o} f(T'')\,d\tau''\right]d\tau' \tag{19}$$

where

$$T' = \tau' - \left(1 - \frac{V_o}{c}\cos^2\theta\right)\tau'' + \frac{V_o}{c}\sin^2\theta\,\frac{\sin\omega\tau''}{\omega} \tag{20}$$

Equations (15), (16), (17), (18), and (20) may be simplified if the factor $\omega\tau$ is assumed to be small. In this case a Taylor series expansion for the sin and cos of $\omega\tau$, including only first and second order terms, is

$$\sin\omega\tau = \omega\tau \tag{21}$$

$$\cos\omega\tau = 1 - \frac{\omega^2\tau^2}{2} \tag{22}$$

The expressions for the Compton currents now become

$$J_r^c(\tau) = -\,eg(r)\,V_o\left[\int_o^{R/V_o} f(T)\,d\tau' - \sin^2\theta\,\frac{\omega^2}{2}\int_o^{R/V_o}\tau'^2 f(T)\,d\tau'\right] \tag{23}$$

$$J_\theta^c(\tau) = eg(r)\,V_o\sin\theta\cos\theta\,\frac{\omega^2}{2}\int_o^{R/V_o}\tau'^2 f(T)\,d\tau' \tag{24}$$

$$J_\phi^c(\tau) = -\,eg(r)\,V_o\sin\theta\,\omega\int_o^{R/V_o}\tau' f(T)\,d\tau' \tag{25}$$

$$T = \tau - (1 - \beta)\,\tau' \tag{26}$$

where $\beta = \frac{V_o}{c}$.

In a like manner Eq (20) becomes

$$\tau' = \tau'' - (1 - \beta)\, \tau''' \tag{27}$$

An expression for the conductivity may also be found by using the equation of motion for the secondary electrons. These electrons are in the thermal regions with energies ranging from about 10-15 eV to the ambient energy. It should be remembered for later use that the ambient energy of the secondary electrons is dependent on the electric field present. For consideration here, it is assumed that $\gamma \gtrsim 1$ and also that the change of velocity with time is small compared to the other terms in Eq (9) so that $\frac{d\vec{V}}{dt}$ may be neglected. Also, with low velocities, the $\vec{V} \times \vec{B}$ term is small compared to the remaining terms and may also be neglected. Then the velocity of the secondary electrons is

$$\vec{V} = - \frac{e}{m\nu_c} \vec{E} \tag{28}$$

Using Eq (28), the current due to the secondary electrons is

$$\vec{J}^s(\tau) = - e \vec{V} n_s(\tau) = \frac{e^2}{m\nu_c} \vec{E}\, n_s(\tau) \tag{29}$$

Comparing Eq (29) to $\vec{J}^s = \sigma\vec{E}$, an expression for the conductivity is

$$\sigma(\tau) = \frac{e^2}{m\nu_c} n_s(\tau) \tag{30}$$

Equations (19), (23), (24), (25), (26), (27), and (30) provide the desired expressions for the Compton currents and the conductivity.

Field Equations

Maxwell's equations is rationalized MKS units are

$$\vec{\nabla} \times \vec{E} = -\frac{\partial \vec{B}}{\partial t} \tag{31}$$

$$\vec{\nabla} \times \vec{B} = \mu_0 \vec{J} + \frac{1}{c^2}\frac{\partial \vec{E}}{\partial t} \tag{32}$$

$$\vec{\nabla}\cdot\vec{E} = \frac{q_v}{\varepsilon_0} \tag{33}$$

$$\vec{\nabla}\cdot\vec{B} = 0 \tag{34}$$

where q_v is the total charge density and $\vec{J}$ is the total current density. In addition to these equations the continuity of charge requires that

$$\frac{\partial q_v}{\partial t} + \vec{\nabla}\cdot\vec{J} = 0 \tag{35}$$

Combining these equations to separate $\vec{E}$ and $\vec{B}$ and transforming them into spherical coordinates and into the retarded time frame (Ref 3) the relations for $\vec{E}$ and $\vec{B}$ become

$$-\nabla^2\vec{E} + \hat{u}_r \frac{1}{c\varepsilon_0}\vec{\nabla}\cdot\vec{J} + \frac{1}{\varepsilon_0}\vec{\nabla}q_v + \frac{\partial}{\partial\tau}\left[\frac{2}{c}\frac{1}{r}\frac{\partial}{\partial r}(r\vec{E}) + \mu_0(\vec{J} - \hat{u}_r J_r)\right] = 0 \tag{36}$$

$$-\nabla^2\vec{B} - \mu_0\vec{\nabla}\times\vec{J} + \frac{\partial}{\partial\tau}\left[\frac{2}{rc}\frac{\partial}{\partial r}(r\vec{B}) + \frac{\mu_0}{c}(\hat{u}_\phi J_\phi - \hat{u}_\theta J_\theta)\right] = 0 \tag{37}$$

In the Karzas-Latter model, only the time derivative portion of Eqs (36) and (37) are kept since the current variation with distance is slow compared to the variation in time for the high frequency com-

ponents. Also the fields and currents vary rapidly in time. This approximation is valid for about 100 shakes. Th s same high frequency approximation is used here. In addition, the radial component of the field is dropped since it is weak compared to the transverse components and contributes only a very low frequency signal (Ref 2). The equations for the transverse components are

$$\frac{\partial}{\partial\tau}\left[\frac{2}{c}\frac{1}{r}\frac{\partial}{\partial r}(rE_{\theta,\phi}) + \mu_0 J_{\theta,\phi}\right] = 0 \tag{38}$$

$$\frac{\partial}{\partial\tau}\left[\frac{2}{c}\frac{1}{r}\frac{\partial}{\partial r}(rB_{\theta}) - \frac{\mu_0}{c} J_{\phi}\right] = 0 \tag{39}$$

$$\frac{\partial}{\partial\tau}\left[\frac{2}{c}\frac{1}{r}\frac{\partial}{\partial r}(rB_{\phi}) + \frac{\mu_0}{c} J_{\theta}\right] = 0 \tag{40}$$

The currents in Eqs (38), (39), and (40) are total currents. The total currents are given by

$$J_{\theta,\phi} = J^c_{\theta,\phi} + \sigma(\tau)\ E_{\theta,\phi} \tag{41}$$

Substitution of Eq (41) into Eqs (38), (39), and (40) and integration over time gives

$$\frac{2}{c}\frac{1}{r}\frac{\partial}{\partial r}(rE_{\theta}) + \mu_0 J^c_{\theta} + \mu_0\ \sigma(\tau)\ E_{\theta} = 0 \tag{42}$$

$$\frac{2}{c}\frac{1}{r}\frac{\partial}{\partial r}(rE_{\phi}) + \mu_0 J^c_{\phi} + \mu_0\ \sigma(\tau)\ E_{\phi} = 0 \tag{43}$$

$$\frac{2}{c}\frac{1}{r}\frac{\partial}{\partial r}(rB_{\theta}) - \frac{\mu_0}{c} J^c_{\phi} - \frac{\mu_0}{c}\ \sigma(\tau)\ E_{\phi} = 0 \tag{44}$$

$$\frac{2}{c}\frac{1}{r}\frac{\partial}{\partial r}(rB_{\phi}) + \frac{\mu_0}{c} J^c_{\theta} + \frac{\mu_0}{c}\ \sigma(\tau)\ E_{\theta} = 0 \tag{45}$$

Equations (42) and (43) are in a form which can be solved. The terms needed for solution of these equations are the air conductivity and the transverse components of the Compton currents. The air conductivity may be found by using Eqs (19) and (30). The transverse components of the Compton currents may be found by using Eqs (24) and (25).

III. Model Considerations

General

While the basic relationship expressions have been developed between $\vec{E}$, $\vec{J}$, and σ, some additional considerations are necessary in developing the presented model. These include such items as the form of the function $f(t)$, the average energies of the gamma rays and Compton electrons, the mean free path of the gamma rays and the range of the Compton electrons, and the collision frequency of the secondary electrons. The validity of the small angle approximation must also be examined. Each of these will be discussed separately in this section.

When all of the items discussed in this section are combined with the equations given in the previous section, one obtains a straightforward and simple calculational model for predicting EMP environments from high altitude nuclear bursts.

Time Dependence of Gamma Rays

Many functions have been proposed to describe the time dependent output of a nuclear weapon, $f(t)$. These pulse shapes are often taken to be of the form (Ref 4)

$$f(t) = \exp\left(-\frac{\alpha}{t} - \beta t\right) U(t) \tag{46}$$

where $U(t)$ is a unit step function having a value zero for negative arguments and unity for all others, and α and β are constants describing the rise and fall of the pulse. Another form often used (Ref 5) is

$$f(t) = \frac{(\alpha + \beta) \exp \alpha (t - t_o)}{\beta + \alpha \exp [(\alpha + \beta)(t - t_o)]} \tag{47}$$

where t_o is the position of the peak value of the function. One feature of these functions is that they cannot be integrated in closed form, and thus EMP codes which use the functions involve time consuming numerical integration schemes for calculating the Compton currents and the atmospheric conductivity.

A basic idea in this investigation was to select functional forms of f(t) that could be integrated directly, thus yielding substantial savings in computation time. There are two constraints that the functional form of f(t) should follow. The first constraint is that the function be integrable in closed form. A second constraint is that the function should match reasonably well those currently in use for EMP calculations.

Since each of the functions given in Eqs (46) and (47) has an exponential rise and decay, prime consideration was given to functions having these same characteristics. With this in mind, the field was narrowed down to the following normalized functions:

$$f(t) = \frac{\alpha\beta}{\beta - \alpha} [\exp(-\alpha t) - \exp(-\beta t)]\, U(t) \tag{48}$$

$$f(t) = \frac{1}{N} \begin{cases} [\exp(\beta t) - 1]\, U(t), & t \le t_o \\ [\exp(\beta t_o) - 1]\, [\exp - \alpha(t - t_o)]\, U(t - t_o) \end{cases} \tag{49}$$

where N is a normalization constant.

It should be apparent at this point that the first constraint given could not be met without the simplification made to Eqs (16), (17), (18), and (20) by the small angle approximations in Eqs (21) and (22).

After further study, it was determined that Eq (48) would fit the functions given in Eqs (46) and (47) closely except for very narrow pulses. Figure 2 shows the shape of a typical long pulse. It is a plot of Eq (48) with $\alpha = 10^7$ and $\beta = 3.7\ (10)^8$. The X marks indicate the values computed from Eq (46) with $\alpha = 10^{-9}$ and $\beta = 10^7$. Figure 3 shows a plot of a typical narrow pulse. In this case, Eq (48) with $\alpha = 2\ (10)^9$ and $\beta = 3\ (10)^8$, and Eq (46) with $\alpha = 2\ (10)^{-8}$ and $\beta = 2\ (10)^8$ were used. The values from Eq (46) are again annotated by X marks. The curve computed from Eq (48) has been shifted in time away from the origin in order for the peaks of the two functions to match. This was done for an easier comparison. The result of this manipulation is to offset the times in the final calculations by the amount necessary to shift Eq (48). In both Figs. 2 and 3, the functions were normalized to a peak value of one for comparison purposes.

Equivalent comparisons using Eq (49) in place of Eq (48) indicated that Eq (48) would give a better overall versatility. Thus Eq (48) was chosen as the pulse shape for the sample calculations of this EMP model.

Energies

Two energy values are needed in the model, that of the gamma rays and that of the Compton electrons. Karzas and Latter (Ref 2) suggest a 1 MeV gamma and a 1 MeV Compton recoil energy. This implies no energy loss in the Compton creation process. Chapman (Ref 3) uses 1.5 MeV gamma rays and 1.28 MeV Compton electrons, which are the most energetic available from 1.5 MeV gamma rays. The values used in the AFWL models vary somewhat (Ref 4), but the most common value appears to be 1.5 MeV gamma rays and .75 MeV Compton electrons. These Compton electron energies are actually the kinetic energy transferred to the elec-

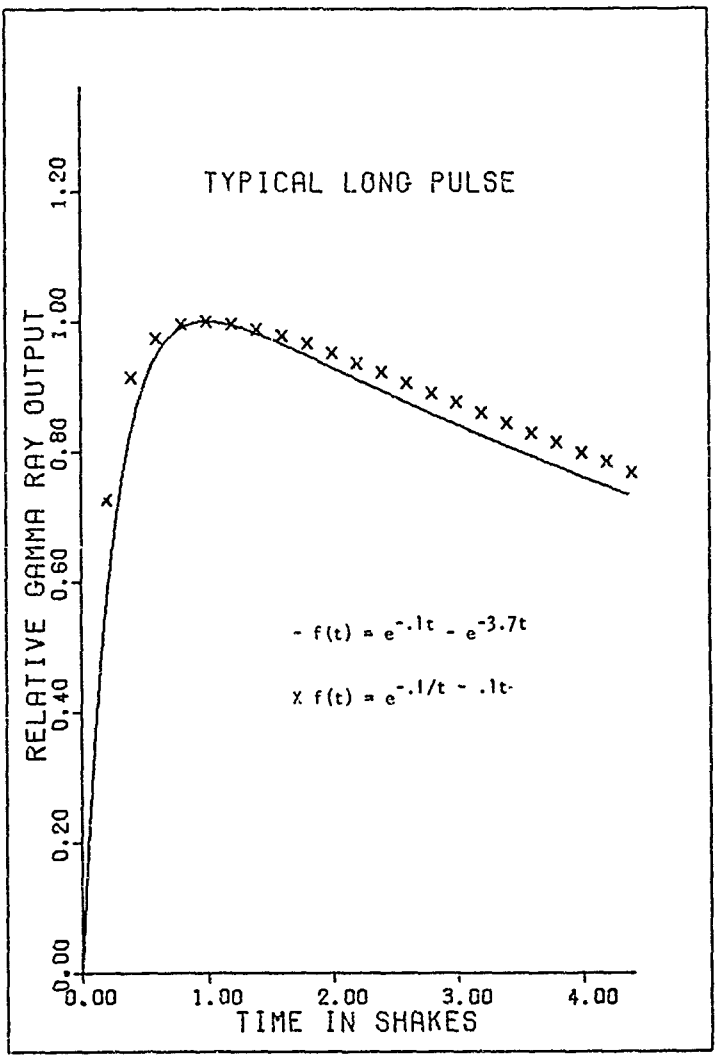


Fig. 2. Typical Long Gamma Output Pulse

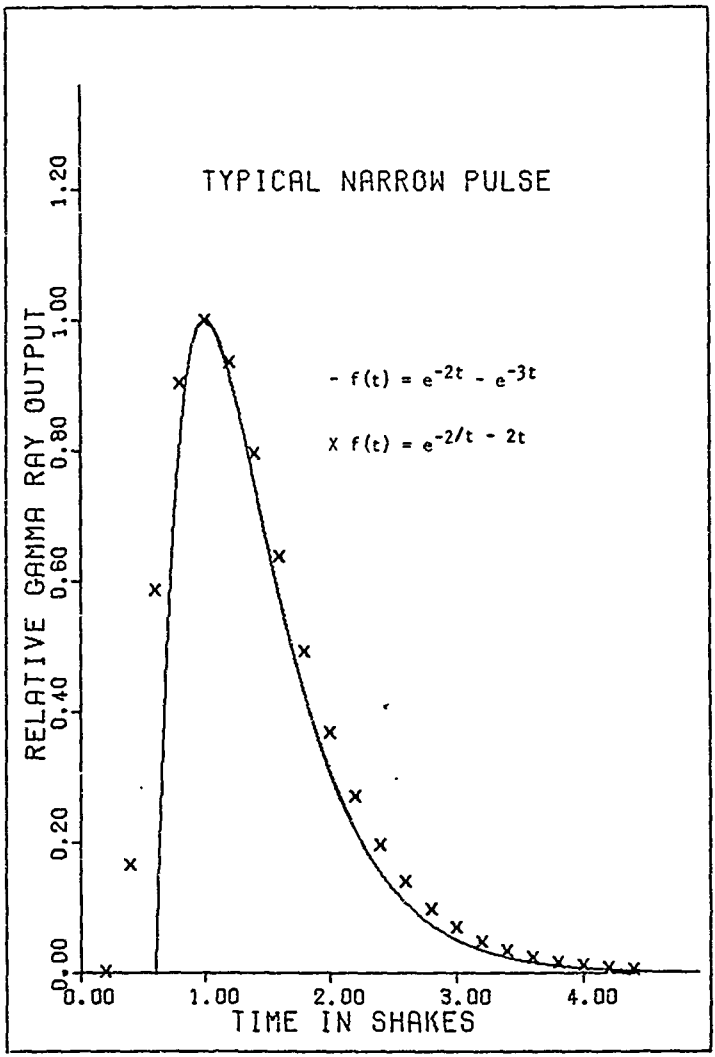


Fig. 3. Typical Narrow Gamma Output Pulse

tron from the gamma ray and assume the Compton electrons are only scattered forward. The energy of .75 MeV from a 1.5 MeV gamma ray corresponds to the average energy transfer in a Compton creation process (Ref 6). This Compton electron energy is given by

$$T = (1 - \sigma_s/\sigma_c)\ h\nu \tag{50}$$

where

T = average recoil energy

σ_s = average Compton scattering (non-absorption) cross section

σ_c = average Compton collision (total interaction) cross section

$h\nu$ = energy of the gamma ray

The values of σ_s and σ_c are from the Klein-Nishina formulas (Ref 6).

With these considerations, 1.5 MeV gamma rays are assumed while the Compton energy is left as a variable.

A question directly related to the energies is that of gamma mean free path and Compton range. The mean free path is defined as the inverse of the total cross section. For Compton creation the total macroscopic cross section is the number of electrons times the absorption microscopic cross section. The absorption cross section is the difference between the collision (total interaction) and scattering cross sections. Using this definition, the mean free path varies little for gamma energies between 1 and 1.5 MeV (Ref 6) so that the value suggested by Karzas and Latter of 300 m at standard pressure is a realistic value and is used in the model.

Katz and Penfold (Ref 7) give relationships between electron energy and range in any material. For electrons with energies less than 2.5 MeV the relationship is

$$R = [412\ E_o^{(1.265\ -\ 0.0954\ \ln E_o)}]/D \qquad (51)$$

where R is the range in cm, E_o is the energy in MeV of the electron, and D is the density in mg/cm^3 of the material of interest. For a .75 MeV electron and an air density of 1.293 mg/cm^3 at standard pressure, the range is 2.23 m. For a 1 MeV electron the range is 3.18 m, which shows an increase of almost one meter. Since the Compton recoil energy is taken as a variable and the range variation is considerable, Eq (51) with an air density of 1.293 mg/cm^3 is used in the model to compute the range of the Compton electrons at standard pressure.

Another factor which is a function of Compton electron energy is the velocity of the Compton electrons. The energy used for the Compton electron is considered to be the kinetic energy of the electron. The total energy is the sum of the kinetic and rest energies. The relativistic relation here is

$$E + m_o = m_o\gamma \qquad (52)$$

where E is the kinetic energy in eV and m_o is the rest energy in eV. Equation (52) may be solved for the Compton electron velocity to get

$$V_o = c\left[1 - \left(\frac{m_o}{E + m_o}\right)^2\right]^{\frac{1}{2}} \qquad (53)$$

Equation (53) is also used in the model.

The energy from the prompt gamma rays is assumed to be deposited in an absorption region from 20 Km to 50 Km above the earth's surface. This is based on calculations by Latter and LeLevier (Ref 8).

Compton Electron Lifetime

The lifetime of a Compton electron, as previously defined, is given by the quotient of the electron range R and its constant speed V_o. The range at any given altitude is found by exponentially scaling the standard pressure value found from Eq (51) and the sea level air density. Since the high frequency approximation is only valid for about 100 shakes, the lifetime should not be allowed to exceed this length of time.

Small Angle Approximation

One important factor for this model is the validity of the small angle approximations leading to Eqs (24), (25), (26), and (27). This can be somewhat arbitrary, depending on the amount of error one is willing to accept. For the use of this analysis, a 2% error will be considered acceptable. With this limit the maximum value for the solution of sin A = A is A = .34.

The maximum geomagnetic field in the gamma ray absorption region is usually taken to be a .6 gauss (Ref 4). A minimum kinetic energy of .5 MeV will be assumed for the Compton electrons. The time which satisfies

$$\omega\tau = .34 \tag{54}$$

is the maximum time duration over which the small angle approximation is valid.

Equation (13) gives the expression for ω. This will be a maximum when B_o is a maximum and γ is a minimum. For γ to be a minimum, the particle speed must be a minimum. The speed of a .5 MeV electron is .863c. With these factors ω is $5.33\ (10)^6$. Solving for τ in Eq (54),

the result is $\tau = 6.4$ shakes. This is however a very worst case. In most situations the electron energy will be considerably greater than .5 MeV. For an electron of .75 MeV with a speed of .9142c, the time limit is $\tau = 7.9$ shakes. If the geomagnetic field is .3 gauss, which is often the case, the time limits above will be doubled.

The minimum length of the confidence interval should be 6.4 shakes. As the electron energy increases, the length of the confidence interval will also increase.

Electron Collision Frequency

In previous EMP models two general approaches have been taken to find a value for the air conductivity. The first uses Eq (30) and assumes a constant collision frequency scaled to an exponential atmosphere. This approach tends to limit the usefulness to a rather narrow range of gamma yields if accurate answers are desired. This basic approach is the one suggested by Karzas and Latter.

The second approach is the use of the electron transport equations (Ref 9) to solve for the secondary electron velocity. This velocity is then used to compute the secondary currents directly. These equations however, require an iterative solution which is very time consuming.

Since the model developed here is desired to be as simple as possible to use and understand, but still give good results over as wide a range of gamma yields as possible, an intermediate approach is desirable.

When a secondary electron is created, it has an energy somewhat higher than its ambient energy. The secondary electrons transfer this additional energy to air molecules through both elastic and inelastic collisions. The time required for this process to take place is known

as the thermalization time. Baum (Ref 10) has gathered data to show that the thermalization time for low energy (about 10 eV or less) electrons at sea level is approximately a nanosecond. Using an exponential atmosphere model, this thermalization time corresponds to approximately 2 shakes at 20 Km and to over a microsecond at 50 Km. The thermalization time in the 20 Km case is on the same order as the time scale of interest (a few shakes) for the high altitude EMP problem. The scale height used for the exponential atmosphere is taken as 7 Km. This value is based on a curve fit of data from the U.S. Standard Atmosphere of 1962 (Ref 11). This scale height of 7 Km is used throughout the model.

Baum also shows the effect of an applied electric field on the ambient electron energy. The secondary electron ambient energy increases with increasing field strengths above 10^4 volts/m. For electric field strengths below 10^4 volts/m there is little or no effect.

If the thermalization process is assumed to be a linear function of time and the lower energy limit of the secondary electrons is assumed to be a linear function of the electric field strength, these effects can be easily incorporated into the EMP model being developed. It is however, necessary to determine the coefficients of the assumed functions.

The time dependent function is based on the thermalization time at 20 Km. The coefficients for the electric field dependent function are based on an empirical fit to the peak electric field values from the AFWL CHEMP model (Ref 4). In order to get an acceptable fit, it was found that the field dependent function had to be split into two linear functions. Since the electron energy and collision frequency are directly related (Ref 9), the linear relations described above may

be expressed directly as electron collision frequency. The functions described are

$$\nu = -2.5\ (10)^{20}\ \tau + 4.5\ (10)^{12} \tag{55a}$$

$$\nu = 0.43\ (10)^{8}\ E + 1.6\ (10)^{12} \qquad E \leq 5\ (10)^{4} \tag{55b}$$

$$\nu = 6\ (10)^{7}\ E + 0.8\ (10)^{12} \qquad E > 5\ (10)^{4} \tag{55c}$$

where τ is retarded time in seconds and E is the electric field strength in volts per meter.

The collision frequency at sea level is taken as the maximum of Eqs (55) and $2.8\ (10)^{12}$. In no case is the collision frequency allowed to exceed $4.4\ (10)^{12}$. The collision frequency is then scaled using an exponential atmosphere. The lower limit value of $2.8\ (10)^{12}$ was determined empirically while the upper limit value of $4.4\ (10)^{12}$ results from the collision frequency being essentially independent of the electric field for extremely high fields (Ref 2).

Preionization

The problem of preionization by a precursor burst may be handled quite easily by the model developed here. This is because of the choice of the gamma yield function of Eq (48) and the small angle approximations of Eqs (21) and (22), which allows Eq (19) to be integrated in closed form to get the number of secondary electrons as a function of retarded time for any altitude. The total air conductivity for a burst with a precursor burst is computed from the total number of secondaries from both bursts at the time of interest. The collision frequency should be based on the time since the precursor burst and the electric field strength due to the main burst at the time of interest.

it is in the calculation of the number of secondary electrons from a precursor burst where the time confidence limit of the small angle approximations is greatly exceeded. The term of interest here is $\frac{\sin \omega\tau''}{\omega}$ in Eq (20). Since this term and its small angle approximation τ'' both have maximums on the order of 10^{-6}, and recombination is a noticeable factor, on preionization time scales, any error introduced by the small angle approximation should be tolerable.

Calculation Method

The time development of the EMP signal may be found by the numerical integration of Eqs (42) and (43) over the absorption region along the line of sight between the burst point and the target for retarded times from 0 to τ. The distance from the burst point to the top of the absorption region along the line of sight is called RMIN while the corresponding distance to the bottom of the absorption region is called RMAX. The distance to the target from the burst point is r. It should be noted that above and below the absorption region there are no currents or air conductivity so that the only contribution to the electric field is over the absorption region. The integration limits are then RMIN and RMAX as shown in Fig. 1 on page 5. RMAX will equal r if the target is in the absorption region.

Because a numerical integration is necessary, this model is best run on a computer. The results given in this report were calculated through a computer code using the concepts and methods detailed here applied to the theory given previously. The computer code calculation will be referred to as HAEMP in the next section.

For points below the absorption region, where both the Compton currents and air conductivity are zero, Eqs (42) and (43) have solu-

$$\frac{2}{c}\frac{1}{r}\left|\frac{\partial}{\partial r}\left(r\,E_{\xi,\phi}\right)\right| << \mu_0\left|J_{\theta,\phi}\right| \tag{59}$$

$$\frac{2}{c}\frac{1}{r}\left|\frac{\partial}{\partial r}\left(r\,E_{\theta,\phi}\right)\right| << \mu_0\,\sigma(\tau)\,E_{\theta,\phi} \tag{60}$$

hold, the first term in Eqs (42) and (43) may be neglected and they reduce to

$$E_\theta = -J_\theta^c/\sigma(\tau) \tag{61}$$

$$E_\phi = -J_\phi^c/\sigma(\tau) \tag{62}$$

the values found from Eqs (61) and (62) may then be used with Eq (53) to find the electric field at the target.

$$\frac{2}{c}\frac{1}{r}\left|\frac{\partial}{\partial r}\left(r\,E_{\xi,\phi}\right)\right| << \mu_0\left|J_{\theta,\phi}\right| \tag{59}$$

$$\frac{2}{c}\frac{1}{r}\left|\frac{\partial}{\partial r}\left(r\,E_{\theta,\phi}\right)\right| << \mu_0\,\sigma(\tau)\,E_{\theta,\phi} \tag{60}$$

hold, the first term in Eqs (42) and (43) may be neglected and they reduce to

$$E_\theta = -J_\theta^c/\sigma(\tau) \tag{61}$$

$$E_\phi = -J_\phi^c/\sigma(\tau) \tag{62}$$

the values found from Eqs (61) and (62) may then be used with Eq (53) to find the electric field at the target.

IV. Results

To test the validity of the NAEMP model, the computed values of this model were compared to available equivalent model values from the AFWL code for EMP calculations known as CHEMP (Ref 4).

The basic set of conditions used for these calculations was:

target location	= ground zero
height of burst	= 100 Km
geomagnetic field	= .3 gauss or 3 $(10)^{-5}$ wb/m^2
inclination angle	= 0.6 degree
Compton electron recoil energy	= .75 MeV

The gamma yield was varied and the number of steps taken for the numerical integration was varied according to the gamma yield, with more steps taken for the higher yields. Other parameters varied for examination of peak field values were burst height, geomagnetic field, and pulse shape. A preionization level was also considered.

The available data from the CHEMP(N) code, which is CHEMP run with non-self-consistent calculations, was computed using a pulse of the form of Eq (46) with $\alpha = 10^{-9}$ and $\beta = 10^{7}$ and the same geometry as given above. This pulse shape is almost identical to that of Eq (48) with $\alpha = 10^{7}$ and $\beta = 3.7\ (10)^{8}$. See Fig. 2 on page 18. Using this pulse shape, a range of gamma yields from .01 Kt to 100 Kt was used to calculate the EMP field values. The peak field values are plotted in Fig. 4. The values taken from the CHEMP(N) code are annotated by X marks. These peak field values show a maximum difference of 5.5% around the 1 Kt case, and a difference of less than 2% for all other known cases.

The complete pulse out to 5 shakes for the .25 Kt case is shown in Fig. 5. Again, values from the CHEMP(M) code are indicated by X marks. There is excellent agreement for the first two shakes after which time the HAEMP values fall off more rapidly. This more rapid fall is most likely caused by two factors. The first is not considering recombination of the secondary electrons, which would tend to reduce the conductivity and allow the fields to fall off more slowly. The second is the slow breakdown of the small angle approximation in computing the Compton currents.

The height of burst was varied to observe the effect on the peak fields for the various yields. This data is plotted in Fig. 6 for altitudes of 60 Km, 100 Km, 200 Km, and 300 Km. The general trend of Fig. 6 indicates that the field strength increases as the height of burst increases only for the larger yields. For the lower yields, the field strength decreases as the burst height increases. Examination of the hypothetical curves in Fig. 6 implies that the maximum EMP signal generated by any given yield depends on the height of burst. For example, using the curves in Fig. 6, it could be concluded that the maximum EMP from a 1 Kt gamma yield would occur for a height of burs somewhere between 60 Km and 200 Km and for a .1 Kt gamma yield, the burst height would be less than 100 Km.

A test was also run to determine the effect of a narrower gamma output pulse. A pulse used by the AFWL in the CHEMP code for this purpose is of the form of Eq (46) with $\alpha = 2\ (10)^{-8}$ and $\beta = 2(10)^{8}$. An essentially identical pulse can be achieved with Eq (48) using $\alpha = 2\ (10)^{8}$ and $\beta = 3\ (10)^{8}$. See Fig. 3 on page 19. A plot of peak fields vs yield is shown in Fig. 7 for both the narrow pulse and the

The complete pulse out to 5 shakes for the .25 Kt case is shown in Fig. 5. Again, values from the CHEMP(M) code are indicated by X marks. There is excellent agreement for the first two shakes after which time the HAEMP values fall off more rapidly. This more rapid fall is most likely caused by two factors. The first is not considering recombination of the secondary electrons, which would tend to reduce the conductivity and allow the fields to fall off more slowly. The second is the slow breakdown of the small angle approximation in computing the Compton currents.

The height of burst was varied to observe the effect on the peak fields for the various yields. This data is plotted in Fig. 6 for altitudes of 60 Km, 100 Km, 200 Km, and 300 Km. The general trend of Fig. 6 indicates that the field strength increases as the height of burst increases only for the larger yields. For the lower yields, the field strength decreases as the burst height increases. Examination of the hypothetical curves in Fig. 6 implies that the maximum EMP signal generated by any given yield depends on the height of burst. For example, using the curves in Fig. 6, it could be concluded that the maximum EMP from a 1 Kt gamma yield would occur for a height of burs somewhere between 60 Km and 200 Km and for a .1 Kt gamma yield, the burst height would be less than 100 Km.

A test was also run to determine the effect of a narrower gamma output pulse. A pulse used by the AFWL in the CHEMP code for this purpose is of the form of Eq (46) with $\alpha = 2\ (10)^{-8}$ and $\beta = 2(10)^{8}$. An essentially identical pulse can be achieved with Eq (48) using $\alpha = 2\ (10)^{8}$ and $\beta = 3\ (10)^{8}$. See Fig. 3 on page 19. A plot of peak fields vs yield is shown in Fig. 7 for both the narrow pulse and the

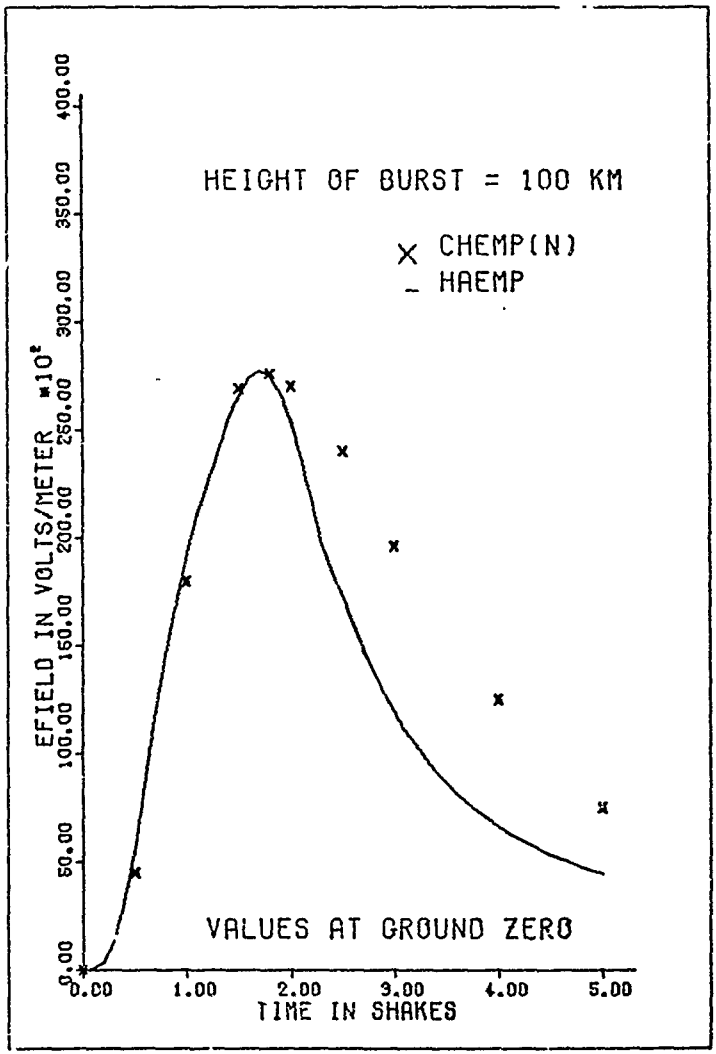


Fig. 5. Electric Field Development for .25 Kt Gamma Burst

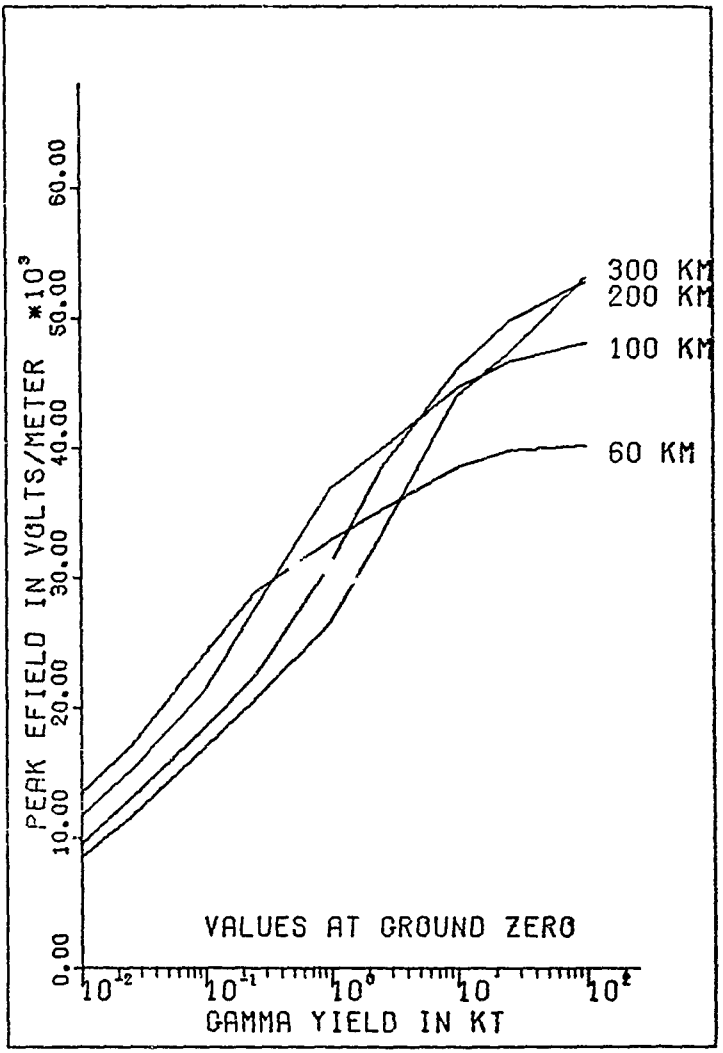


Fig. 6. Peak Electric Field as a Function of Burst Height

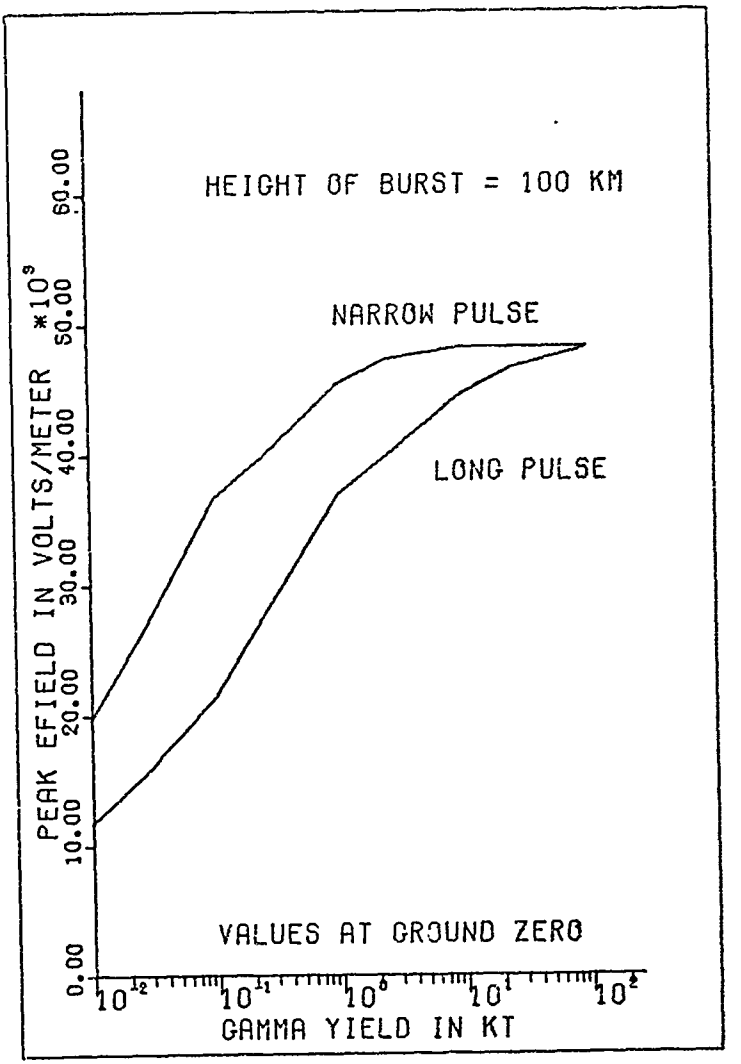


Fig. 7. Peak Electric Fields for Two Gamma Pulse Shapes

original long pulse. This data points to a saturated peak field strength of 4.82 $(10)^4$ volts/m for the 100 Km burst case in a .3 gauss geomagnetic field. The narrow pulse curve shows that the peak fields are higher for all yields. The data from Fig. 6 however shows that the saturated field value predicted in Fig. 7 does not hold for all burst heights.

Another factor which should have a noticeable effect on the EMP generated is the presence of a precursor burst. For this test a .03 Kt gamma yield burst was assumed to have been detonated 10 μsec prior to the main burst. The pulse shape used to describe the gamma output is the initial long pulse and is used for both bursts. The peak field results are plotted in Fig. 8. The results of this test were quite dramatic. This data shows that the peak field of 1.6 $(10)^4$ volts/m from the .03 Kt precursor burst is not equaled until the main burst has a yield of nearly 1 Kt. In general, the peak field values with this level of preionization are the same as if the weapon yield was one tenth of its actual yield. As the yield of the main burst goes up, the field reduction becomes less. At a yield of .1 Kt the field is reduced by over a factor of 4. At .25 Kt the factor drops to 3 and to 2 for the 1 Kt case. When the yield finally reaches 100 Kt, the reduction factor has dropped to 1.1.

The results with preionization compare favorably with available results from the AFWL (Ref 4). However, since a slightly different geometry and some additional source modeling were used, a direct comparison cannot be made.

A last major factor to consider for this model is the geomagnetic field strength. The peak field values as a function of yield are

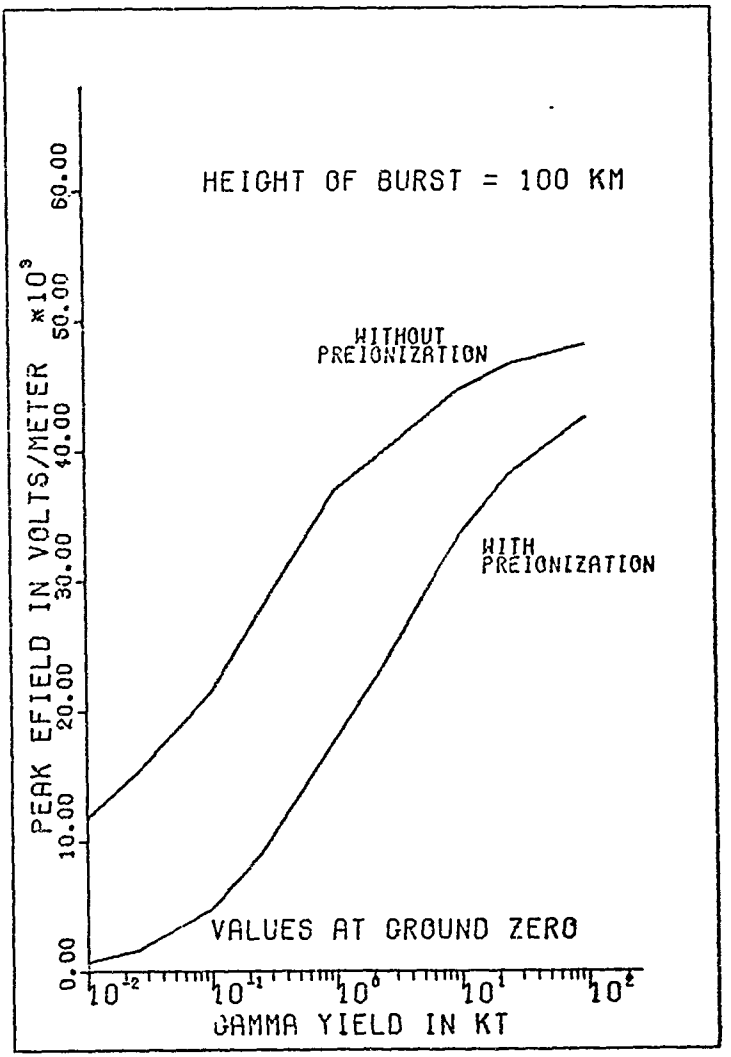


Fig. 8. Effect of a .03 Kt Gamma Yield Precursor Burst

plotted in Fig. 9 for the .3 gauss and the .6 gauss geomagnetic fields. The larger geomagnetic field resulted in approximately a times 2 increase in the field strengths for all yields considered.

One remaining result should be mentioned. This concerns the time of the peak field value. Since for these calculations the fields were computed in steps of .1 shake, the peak field time will be accurate only to this limit. The peak for the .25 Kt case shown in Fig. 5 occurs at 1.7 shakes for the HAEMP model and at an estimated 1.8 shakes for the CHEMP(N) code. As the yield goes up, the peak field value occurs earlier. For yields above .25 Kt, the peak occurs between 1.1 and 1.3 shakes for all cases examined. For all yields and altitudes considered, the peak always occurred within 8 shakes, with the majority falling between 1 and 2 shakes.

Since the model presented is supposed to be a quick computational tool, some estimates on the calculation times that can be expected are appropriate. The times given here are the average times used in computing the results given above and are based on a computer code run on a CDC 6600 computer. The average computation time was 1.5 sec for a 5 shake calculation of the electric field development computed every .1 shake using 50 steps in the numerical integration. Increasing either the parameter of 50 steps or 5 shakes by any factor increased the computation time by the same factor. The presence of a precursor burst had no noticeable effect on computation time. When the approximations of Eqs (61) and (62) were valid, the time dropped to less than .2 sec for a 5 shake calculation.

An interesting observation related to the numerical integration is that as Eqs (61) and (62) become valid, the numerical integration could

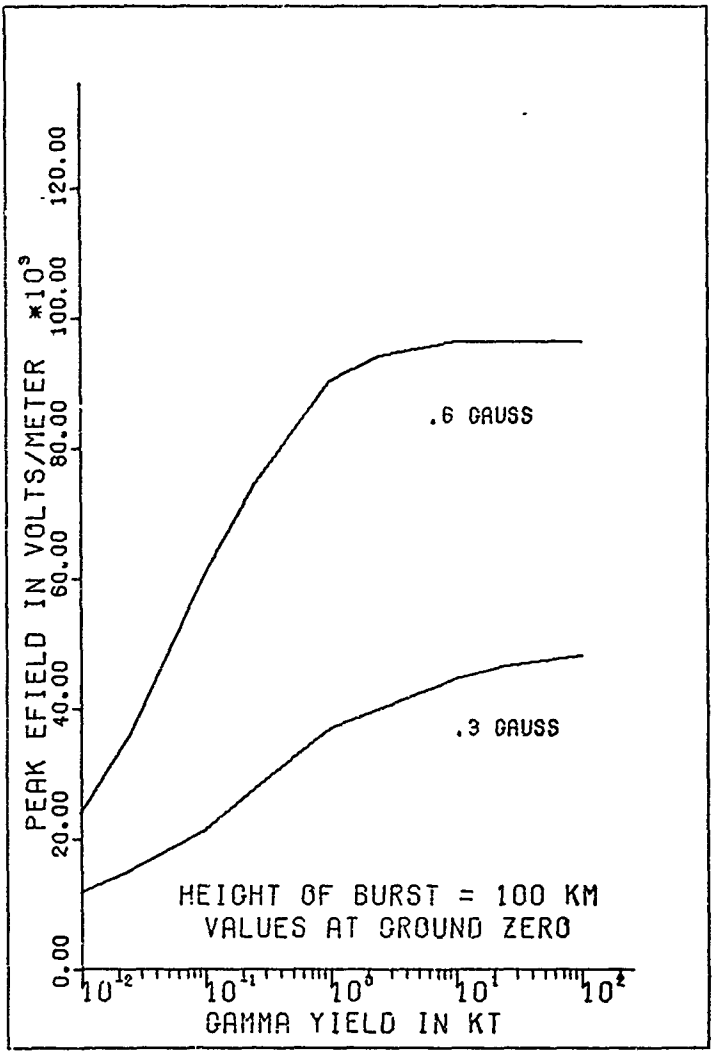


Fig. 9. Effect of Geomagnetic Field Strength on Peak Fields

give unstable results.

V. Conclusions and Recommendations

This report has presented a calculational model for the high altitude EMP. This model falls between the very simple and highly sophisticated models currently available. The model is easy to understand but allows the variation of the major theoretical parameters. The model is also simple enough to use so that a preionization level can be incorporated with a very minimum of effort. The results given by this model are in excellent agreement with the available data from the very sophisticated models using the same geometry. The computation time is on the order of a few seconds.

Uses

There are two primary uses seen for this model. The first is for sensitivity determinations for a given parameter, such as precursor yield in preionization studies, height of burst for a fixed yield, or changes in the magnitude and inclination of the geomagnetic field. Calculations using the HAEMP model can help to evaluate the relative importance of the many variables encountered in EMP problems. It is useful in this role because it gives quick answers which are reasonably accurate.

The second use is as a classroom model. The basic physics of the high altitude problem is present in an easy to use form which demonstrates how the currents, conductivity, and electric field interact with each other. Because the calculations required to get an answer are minimal and straightforward, the physical processes are not lost in the search for a result, as can happen all too easily with highly sophisticated models. Since the results are in relatively good agreement with

the sophisticated models, the student can leave the classroom with a good concept of the overall problem.

Limitations

The model does have its limitations, however. These are due to the various assumptions and approximations used to arrive at the final calculational model. These assumptions and approximations should be kept in mind when using the model. If this is done, the results from any problem can be reasonably interpreted.

Two of the error sources are the small angle approximations and the assumption of a flat earth. For the small angle case the error is negligible at very early times but increases as the time increases. In the flat earth assumption, any error is relatively constant for a particular geometry, but changes when the geometry changes. This error increases as the ground image of the target moves on the earth's surface away from the ground zero point. The other assumptions also add some error to the results, but if the effects of these assumptions are remembered, the HAEMP model can be helpful for the solutions of a wide range of EMP problems.

Recommendations

There are several areas of investigation which might lead to improvements in the HAEMP model. One of the more important possible investigations is to determine if the electron transport equations used in the AFWL CHEMP model to describe the secondary electrons can be greatly simplified and used in the HAEMP model. Another area is the possibility of allowing recombination and cascading of secondary electrons. The use of self-consistent electromagnetic fields is also a possible source

of improvement. This change however would have to be examined very closely to determine the effects it would have on the validity of the small angle approximations, which are vital to the HAEMP model. An additional possibility is the consideration of small angle scattering of the Compton electrons. This could possibly be included by a random elimination of some Compton electrons for Compton current production while still allowing all Compton electrons to produce secondary electrons.

Each possible change to the HAEMP model should be examined with consideration to the tradeoffs between more complete solutions and the continued ease of use and understanding of the model.

Bibliography

1. Kinsley, O.V. Introduction to the Electromagnetic Pulse, Wright-Patterson AFB: Air Force Institute of Technology, March 1971. (GNE/PH/71-4).

2. Karzas, W.J. and R. Latter. "Detection of the Electromagnetic Radiation from Nuclear Explosions in Space", Physical Review, 137-5B:1369-1378 (March 8, 1965).

3. Chapman, T.C. A Computer Code for High Altitude EMP, Wright-Patterson AFB: Air Force Institute of Technology, January 1974. (GNE/PH/74-1).

4. Canavan, G.H., J.E. Brau, L.A. Wittwer. Sensitivity of Self-Consistent High Altitude Electromagnetic Pulse Calculations to Pre-Ionization and Improved Source and Ionization Models. AFWL EMP Theoretical Note 190. Kirtland AFB: Air Force Weapons Laboratory, October 1973.

5. Pomranning, G.C. "Early Time Air Fireball Model for a Near-Surface Burst", DNA 3029T, March 1973.

6. Evans, R.D. The Atomic Nucleus, New York: McGraw Hill Book Co. 1966.

7. Katz, L. and A.S. Penfold. "Range-Energy Relations for Electrons and the Determination of Beta-Ray End-Point Energies by Absorption", Reviews of Modern Physics, 24-1:28-44 (January 1952).

8. Latter, R. and R.E. LeLevier. "Detection of Ionization Effects from Nuclear Explosions in Space", Journal of Geophysical Research, 68-6 (March 15, 1963)

9. Air Force Weapons Laboratory. CHEMP: A Code for Calculation of High-Altitude EMP. AFWL Technical Report 74-49. Kirtland AFB: AFWL, July 1974.

10. Baum, C.E. Electron Thermalization and Mobility in Air. AFWL EMP Theoretical Note 12 (AFWL-EMP 2-1). Kirtland AFB: Air Force Weapons Laboratory, July 1965.

11. U.S. Standard Atmosphere, 1962. Washington DC: U.S. Government Printing Office. December 1962.

12. Carnahan, B., H.A. Luther, J.O. Wilkes. Applied Numerical Methods, New York: John Wiley & Sons, Inc. 1969.

Appendix A

HAEMP Model Summary

HAEMP Model Summary

The user of the HAEMP model must first determine the following parameters in MKS units:

the gamma yield Y of the weapon in MeV.

the height of burst (HOB) of the weapon.

the magnitude B_0 and angle of inclination of the geomagnetic field in the absorption region.

the target location in spherical coordinates with the origin at the burst point and with the polar axis parallel to the geomagnetic field lines.

the kinetic energy E_c of the Compton electrons in MeV.

the parameters defining the gamma output pulse shape.

the atmospheric scale height S to be used.

From these parameters, the values for the angle A and the two distances RMIN and RMAX used for integration over the absorption region can be found from geometry. The angle from the vertical to the line of sight from the burst point to the target is the angle A, as shown in Fig. 1 on page 5. The value of RMIN is the radial distance from the burst point to the top of the absorption layer (50 km above the earth's surface) along the line of sight to the target. The value of RMAX is the corresponding distance to the bottom of the absorption layer (20 Km above the earth's surface). See Fig. 1 on page 5.

The electric field development from times 0 to τ in steps of $\Delta\tau$ in the retarded time frame is found by the numerical integration of

$$\frac{2}{c}\frac{1}{r}\frac{\partial}{\partial r}(rE_\theta) + \mu_0 J_\theta^c + \mu_0 \sigma(\tau) E_\theta = 0 \qquad (42)$$

$$\frac{2}{c}\frac{1}{r}\frac{\partial}{\partial r}(rE_{\phi}) + \mu_0 J^c_{\phi} + \mu_0 \sigma(\tau) E_{\phi} = 0 \tag{43}$$

over r from RMIN to RMAX for each time increment. The initial conditions on these equations are that E_θ and E_ϕ are zero at $\tau = 0$. The number of steps taken over the integration interval will depend on the yield of the weapon and the accuracy desired. No less than 50 steps should be used or more than 500 steps necessary for gamma yields up to 100 Kt.

The solutions to Eqs (42) and (43) will give the electric field components at r = RMAX. The total field strength is given by

$$E = [(E_\theta)^2 + (E_\phi)^2]^{\frac{1}{2}} \tag{63}$$

and the field strength at the target is given by

$$E(\text{target}) = \frac{\text{RMAX}\ E}{r_{\text{target}}} \tag{58}$$

The peak electric field value over the time interval 0 to τ is the maximum value found using Eq (58).

In the special case where the conditions

$$\frac{2}{c}\frac{1}{r}\left|\frac{\partial}{\partial r}(rE_{\theta,\phi})\right| << \mu_0 \left|J^c_{\theta,\phi}\right| \tag{59}$$

$$\frac{2}{c}\frac{1}{r}\left|\frac{\partial}{\partial r}(rE_{\theta,\phi})\right| << \mu_0 \sigma(\tau) E_{\theta,\phi} \tag{60}$$

hold, the electric field components are given by

$$E_\theta = - J^c_\theta/\sigma(\tau) \tag{61}$$

$$E_\phi = - J^c_\phi/\sigma(\tau) \tag{62}$$

The values from Eqs (61) and (62) may then be used with Eqs (53) and (50) to find the electric field at the target.

In order to integrate Eqs (42) and (43) or to compute Eqs (61) and (62), the terms J_θ^c, J_ϕ^c, and $\sigma(\tau)$ are needed as functions of time τ and distance r. These are given by

$$J_\theta^c = eg(r)\, V_c \sin\theta \cos\theta \frac{\omega^2}{2} \int_0^{R/V_o} \tau'^2\, f(T)\, d\tau' \tag{24}$$

$$J_\phi^c = -eg(r)\, V_o \sin\theta\, \omega \int_0^{R/V_o} \tau'\, f(T)\, d\tau' \tag{25}$$

$$\sigma(\tau) = \frac{e^2}{m\nu_c} n_s(\tau) \tag{30}$$

where

$$g(r) = \frac{Y}{E_c} \frac{1}{4\pi r^2 \lambda(r)} \exp\left\{ -\frac{S}{\lambda_o \cos A} \exp -\left(\frac{HOB}{S}\right)\left[\exp\left(\frac{r\cos A}{S}\right) - 1\right]\right\} \tag{3}$$

$$f(T) = \frac{ab}{b-a}\left[\exp(-aT) - \exp(-bT)\right] U(T) \tag{48}$$

$$n_s(\tau) = \frac{qV_o}{R}\, g(r) \int_{-\infty}^{\tau} \left[\int_0^{R/V_o} f(T')\, d\tau''\right] d\tau' \tag{19}$$

$$T = \tau - (1-\beta)\,\tau' \tag{26}$$

$$T' = \tau' - (1-\beta)\,\tau'' \tag{27}$$

with $\beta = \frac{V_o}{c}$ and $q = E_c/33$ eV

The Compton electron cyclotron frequency ω is given by

$$\omega = \frac{eB_o}{m\gamma} \tag{13}$$

The Compton electron velocity V_o is given by

$$V_o = c \left[1 - \left(\frac{m_o}{E_c + m_o} \right)^2 \right]^{\frac{1}{2}} \tag{53}$$

The Compton electron range at sea level is given by

$$R = [412\ E_c^{(1.265\ -\ .0954\ \ln E_c)}]/D \tag{51}$$

where $D = 1.293\ mg/cm^3$. This range is then converted to meters and scaled to the appropriate value for the point r by multiplying the computed value by

$$\exp\ [(HOB - r \cos A)/S] \tag{64}$$

Then the Compton lifetime R/V_o is given by the quotient of the corrected R and V_o, but is never allowed to exceed one usec.

The value of $\lambda(r)$ is given by the product of λ_0 (300 m) and Eq (63).

The collision frequency ν_c at sea level is given by the maximum of

$$\nu_c = -2.5\ (10)^{20}\ \tau + 4.5\ (10)^{12} \tag{55a}$$

$$\nu_c = 0.43\ (10)^8\ E + 1.6\ (10)^{12} \qquad E \leq 5\ (10)^4 \tag{55b}$$

$$\nu_c = 6\ (10)^7\ E + 0.8\ (10)^{12} \qquad E > 5\ (10)^4 \tag{55c}$$

or $2.8\ (10)^{12}$ where τ is the retarded time in seconds and E is the electric field strength in volts per meter. The collision frequency is not allowed to be greater than $4.4\ (10)^{12}$. The value of the collision frequency is recomputed after each time step in the development of the

electric field. The sea level value is also scaled for altitude by dividing by Eq (54).

The integrals in Eqs (24), (25), and (19) can be evaluated in closed form. The step function U(T) in Eq (48) results in two expressions for each of the integrals. The first set of expressions is used when $\tau - (1 - \beta)(R/V_o) \leq 0$ and the second when $\tau - (1 - \beta)(R/V_o) > 0$.

When $\tau - (1 - \beta)(R/V_o) \leq 0$, Eqs (24), (25), and (30) become

$$J_\theta^c(\tau) = eq(r)\, V_o \sin\theta \cos\theta \frac{\omega^2}{2} \frac{1}{b-a} \frac{1}{(1-\beta)^3} \{[(a\tau)^2 - 2a\tau + 2 - 2\exp(-a\tau)] \frac{b}{a^2} - [(b\tau)^2 - 2b\tau + 2 - 2\exp(-b\tau)] \frac{a}{b^2}\} \tag{65}$$

$$J_\phi^c(\tau) = -eq(r)\, V_o \sin\theta\, \omega \frac{1}{b-a} \frac{1}{(1-\beta)^2} \{[a\tau - 1 + \exp(-a\tau)] \frac{b}{a} - [b\tau - 1 + \exp(-b\tau)] \frac{a}{b}\} \tag{66}$$

$$\sigma(\tau) = \frac{e^2 a}{m} q(r) \frac{1}{\nu_c} \frac{V_o}{R} \frac{1}{b-a} \frac{1}{(1-\beta)} \{[a\tau - 1 + \exp(-a\tau)] \frac{b}{a} - [b\tau - 1 + \exp(-b\tau)] \frac{a}{b}\} \tag{67}$$

When $\tau - (1 - \beta)(R/V_o) > 0$, Eqs (24), (25), and (30) become

$$J_\theta^c(\tau) = eq(r)\, V_o \sin\theta \cos\phi \frac{\omega^2}{2} \frac{1}{b-a} \frac{1}{(1-\beta)^3}$$

$$\{\exp(-a\tau)\,[\exp(aL)\,[(\omega L)^2 - 2aL + 2] - 2]\,\frac{b}{a^2} \qquad (68)$$

$$- \exp(-b\tau)\,[\exp(bL)\,[(bL)^2 - 2bL + 2]\,\frac{a}{b^2}\}$$

$$J_\phi^c(\tau) = - eq(r)\, V_o \sin\theta\, \omega \frac{1}{b-a} \frac{1}{(1-\beta)^2}$$

$$\{\exp(-a\tau)\,[\exp(aL)\,[aL - 1] + 1]\,\frac{b}{a} \qquad (69)$$

$$- \exp(-b\tau)\,[\exp(bL)\,[bL - 1] + 1]\,\frac{a}{b}\}$$

$$\sigma(\tau) = \frac{e^2\sigma}{m}\, g(r)\, \frac{1}{\nu_c} \frac{V_o}{R} \frac{1}{b-a} \frac{1}{1-\beta}$$

$$\{\frac{b}{a}\,[aL - 1 + \exp(-aL) - [\exp(aL) - 1][\exp(-a\tau) - \exp(-aL)]]$$

$$- [\frac{a}{b}\,bL - 1 + \exp(-bL) - [\exp(bL) - 1][\exp(-b\tau) \qquad (70)$$

$$- \exp(-bL)]]\}$$

where $L = (1-\beta)(R/V_o)$.

Vita

Louis W. Seiler, Jr. was born on 10 January 1947 in New Orleans, LA. He graduated from high school in New Orleans in 1964. He attended Louisiana State University in New Orleans and received the degree Bachelor of Science, Physics in 1969. He entered the U.S. Air Force Officer Training School in October 1969 and received a commission in December 1969. He served as Group Interactive Computer Systems Analyst in the 4000 Aerospace Applications Group until June 1973 when he entered the Air Force Institute of Technology.

Permanent Address: 3918 Croydon Street
Slidell, LA 70458

This thesis was typed by Katherine Randall